Electronic Supplementary Material (ESI) for Journal of Materials Chemistry A.

Supporting Information

Unprecedented urea oxidation on Zn@Ni-MOF with an ultra-high current density: Understanding toward a competition between UOR and OER, catalytic activity limitation and reaction selectivity

Nabeen K. Shrestha*[,a], Supriya A. Patil[b], Amol S. Salunke[a], Akbar I. Inamdar[a], Hyunsik Im*[,a]

[a]Division of Physics and Semiconductor Science, Dongguk University, Seoul-04620, Republic of Korea.

[b]Department Nanotechnology & Advanced Materials Engineering, Sejong University, Seoul-05006, Republic of Korea.

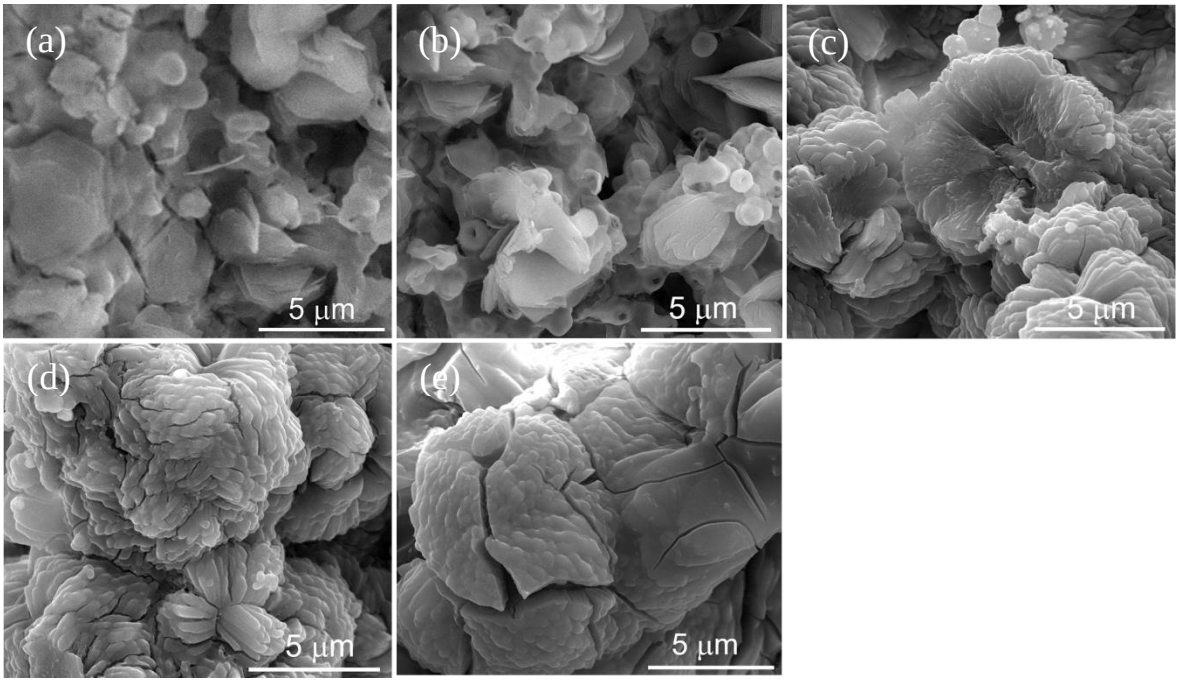

Figure S1. SEM surface views of Ni-MOF with various concentration of Zn-dopant added to the MOF precursor during synthesis. (a) 0, (b) 0.25, (c) 0.5, (d) 0.75 and (e) 1.0 millimoles.

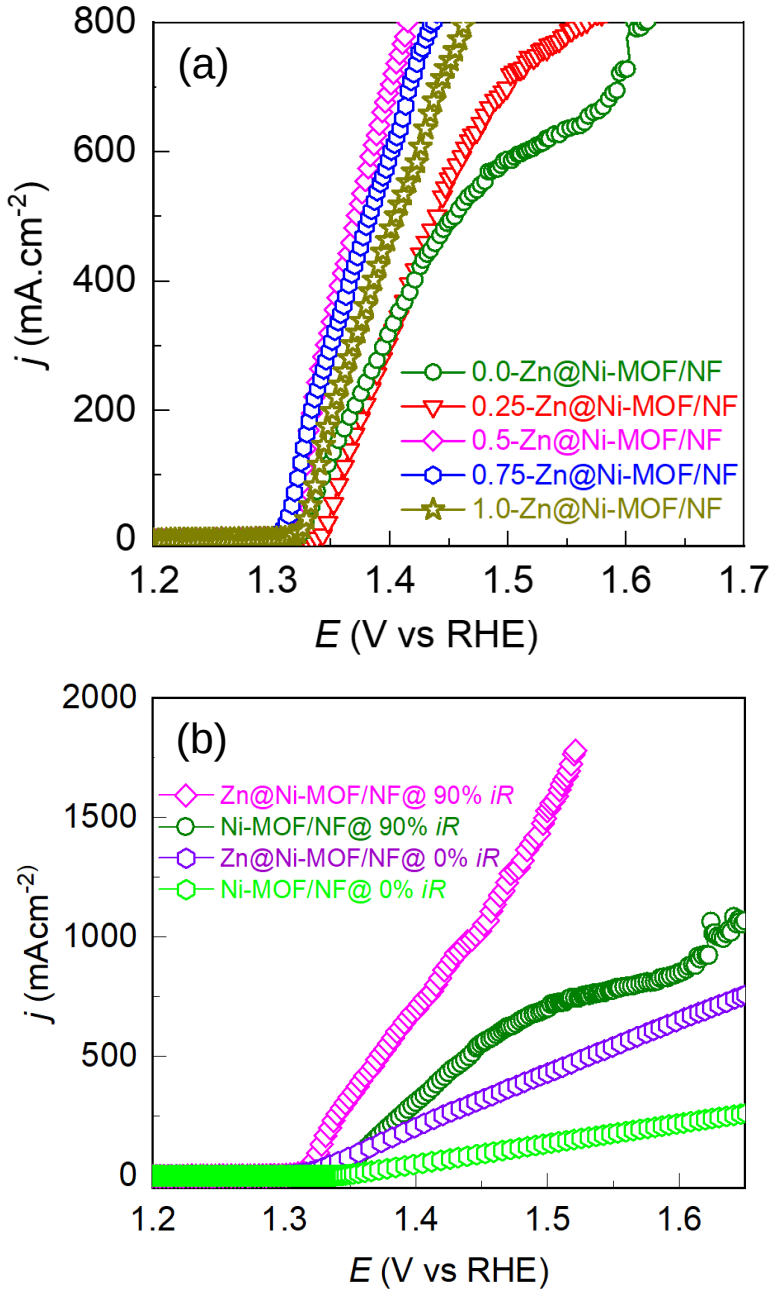

Figure S2. (a) Linear sweep polarization curves recorded at 90% *iR* loss compensation of the Ni-MOF/NF electrode doped with various concentrations of Zn-dopant (as described in figure S1) in 0.33 M urea containing 1.0 M KOH aqueous electrolyte. (b) Linear sweep polarization curves of the Zn@Ni-MOF/NF and Ni-MOF/NF electrodes recorded with and without *iR* loss compensation.

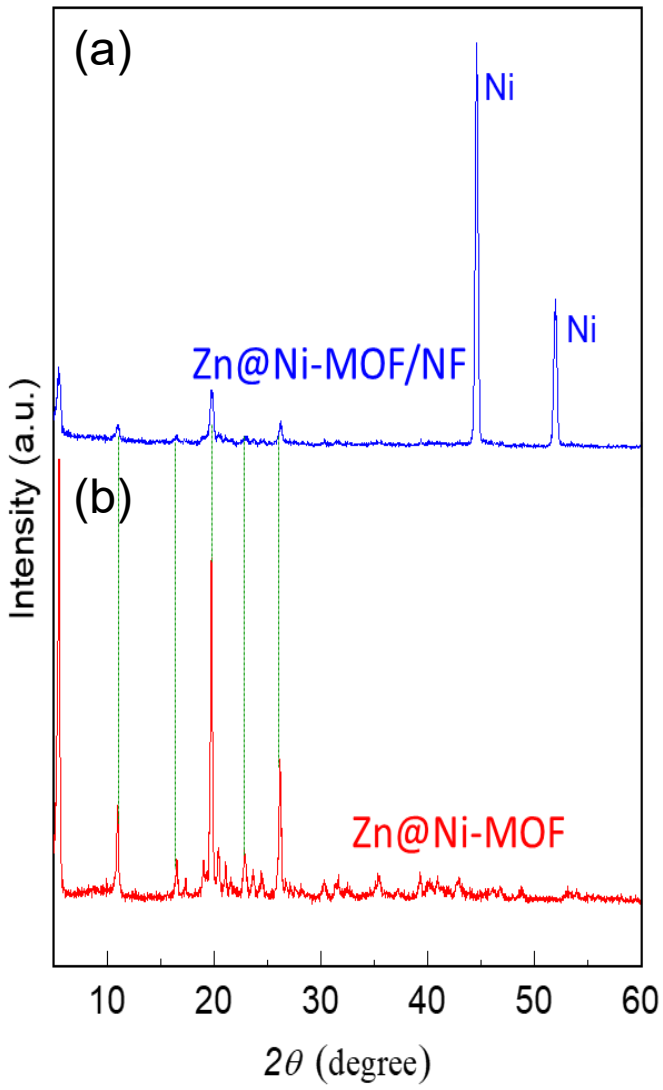

Figure S3. XRD patterns of the Zn@Ni-MOF (a) film deposited on a nickel substrate and (b) bulk powder form.

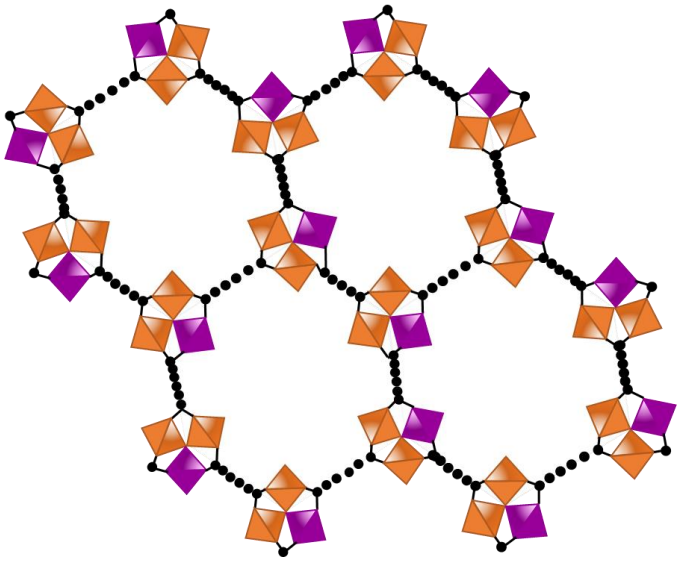

Figure S4. Schematic structure of Zn@Ni-MOF. The purple and orange metal nodes represent the Zn and Ni, respectively coordinating with the organic linker represented by the line of black spheres.

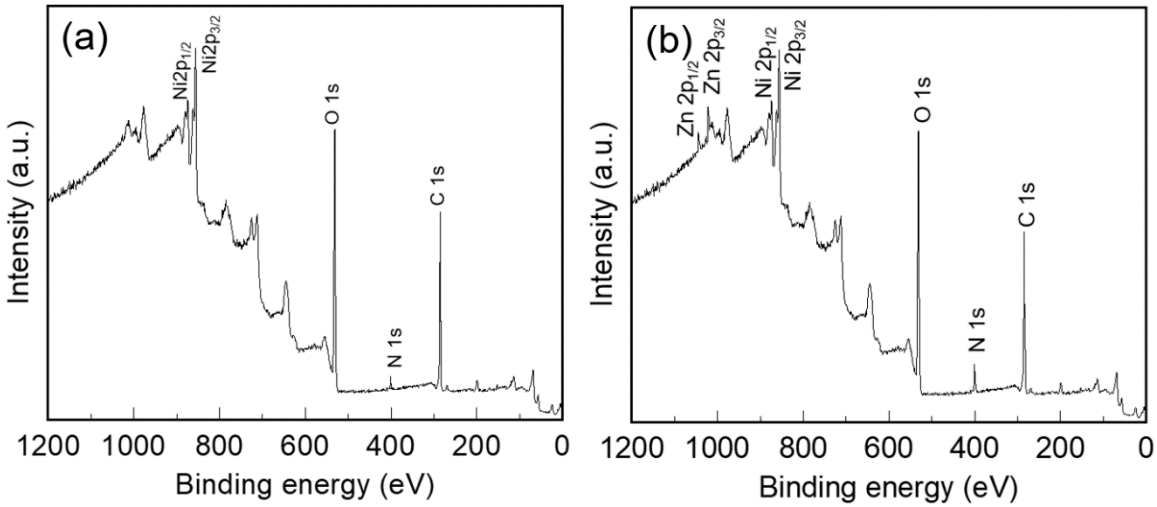

Figure S5. XPS elemental survey spectra of the (a) Ni-MOF/NF and (b) Zn@Ni-MOF/NF samples.

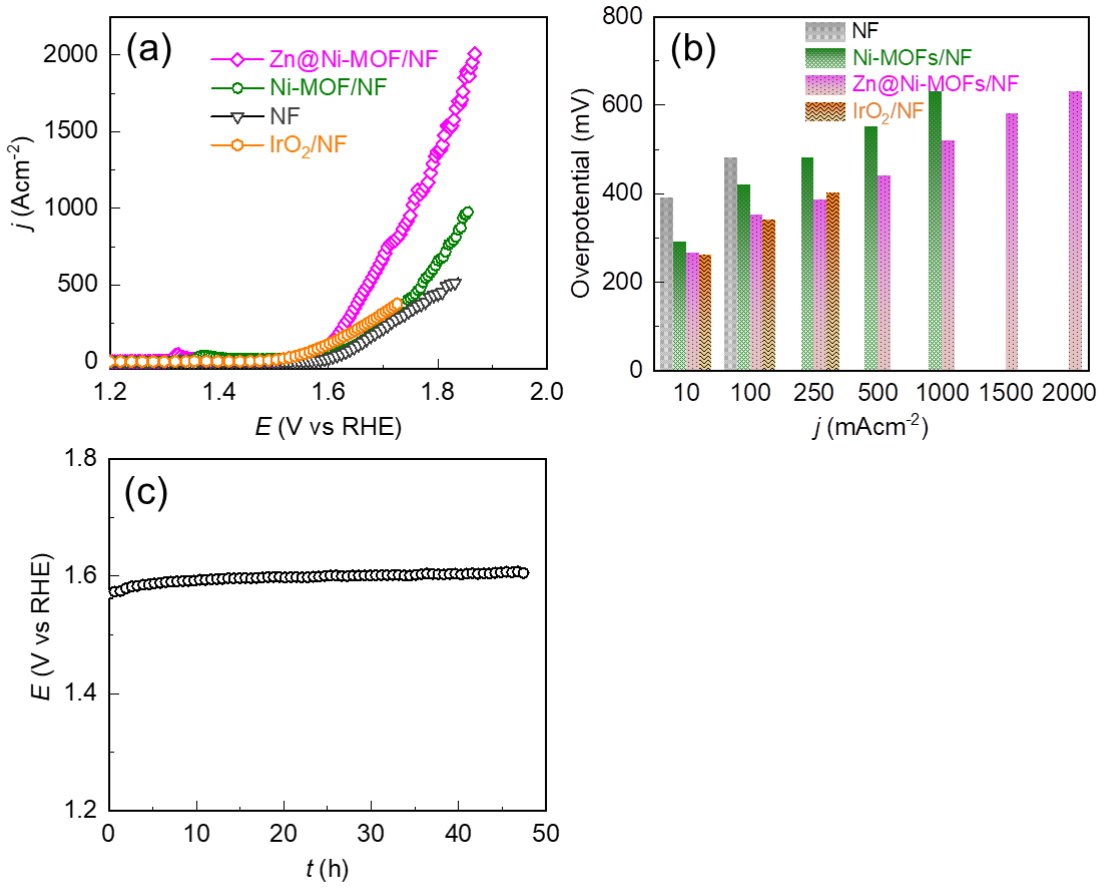

Figure S6. (a) Linear sweep voltammetry curves of various catalytic electrodes in 1.0 M KOH aqueous electrolyte, (b) corresponding OER overpotential verses current density profile, and (c) chronopotentiometric response of the Zn@Ni-MOF/NF sample recorded during the long-term electrochemical stability test for 48 h at 100 $mAcm^{-2}$.

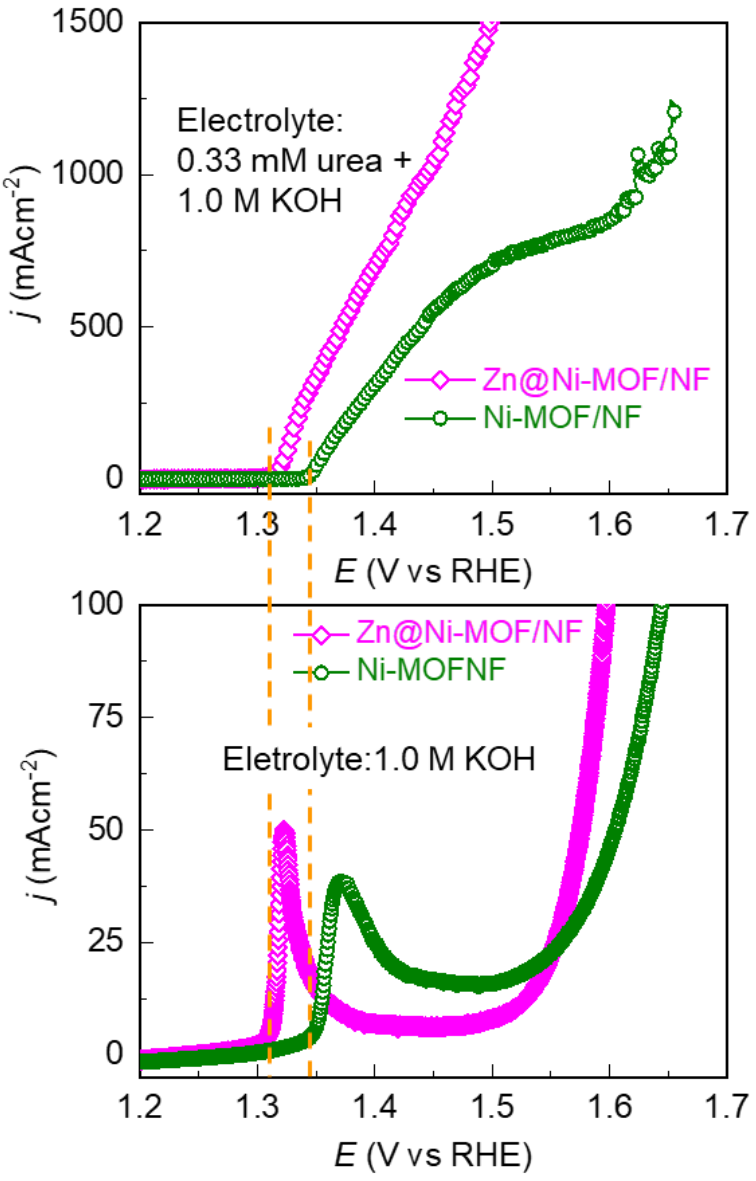

Figure S7. Linear sweep polarization curves of the MOF/NF based electrodes in 1.0 M KOH and 0.33 M urea containing 1.0 M KOH aqueous electrolytes showing the onsets for UOR (upper figure) and Ni^{3+}-OOH phase formation (bottom figure).

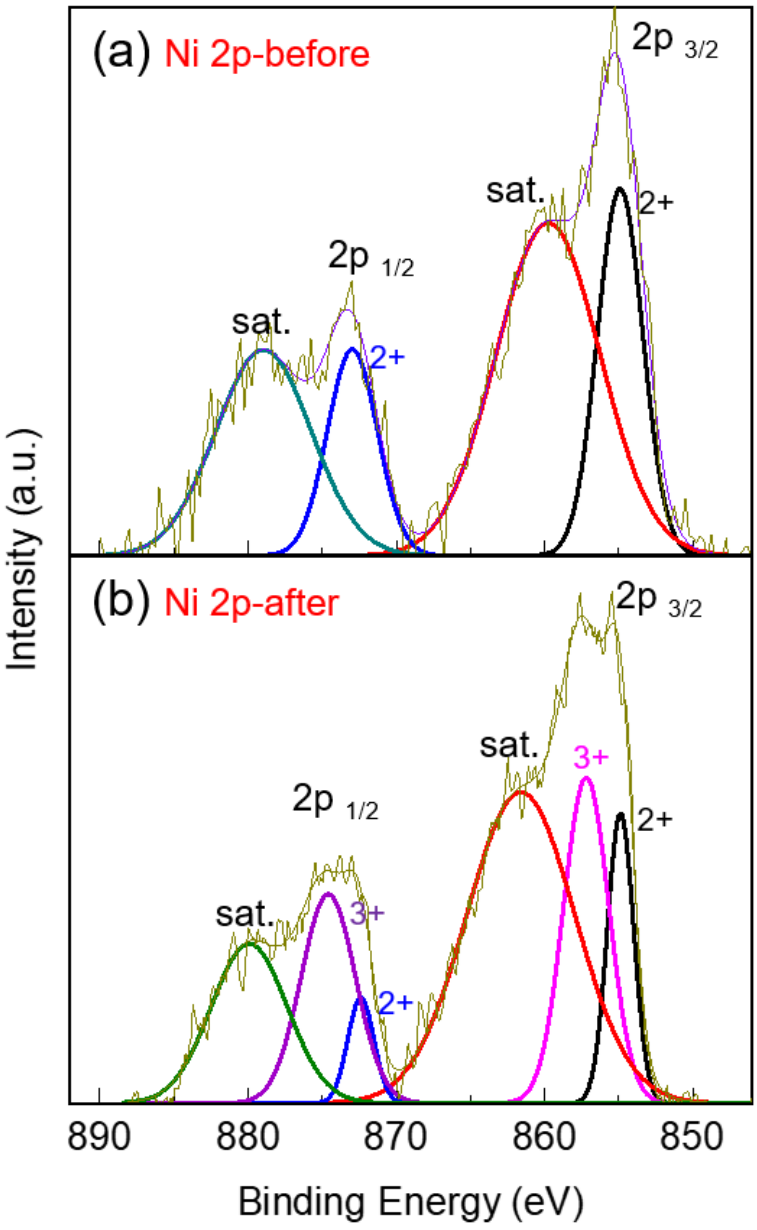

Figure S8. XPS Ni 2p spectra exhibited by the Zn@Ni-MOF/NF anodes recorded (a) before and (b) after electrolyzing 0.33 M urea in 1.0 M KOH aqueous solution for 600 s at 1.40 V vs RHE.

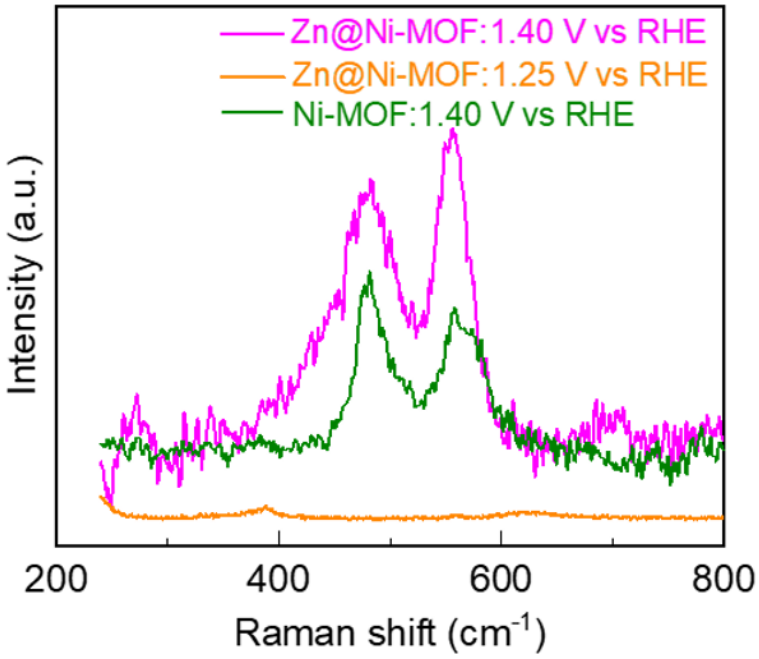

Figure S9. Raman spectra exhibited by the MOF/NF anodes recorded after electrolyzing 0.33 M urea in 1.0 M KOH aqueous solution for 600 s at 1.25 V and 1.40 V vs RHE.

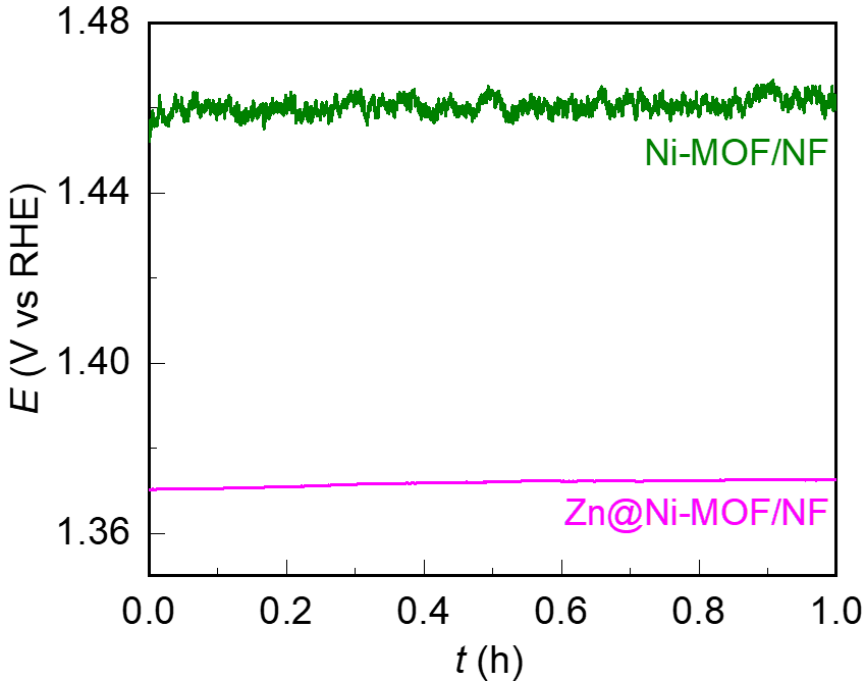

Figure S10. Chronopotentiometric curves exhibited by the MOF/NF based electrodes in 0.33 M urea containing 1.0 M KOH aqueous electrolyte at 100 $mAcm^{-2}$. The Ni-MOF/NF electrode showed the fluctuated curve due to the slower release of the gas bubbles residing on the electrode surface.

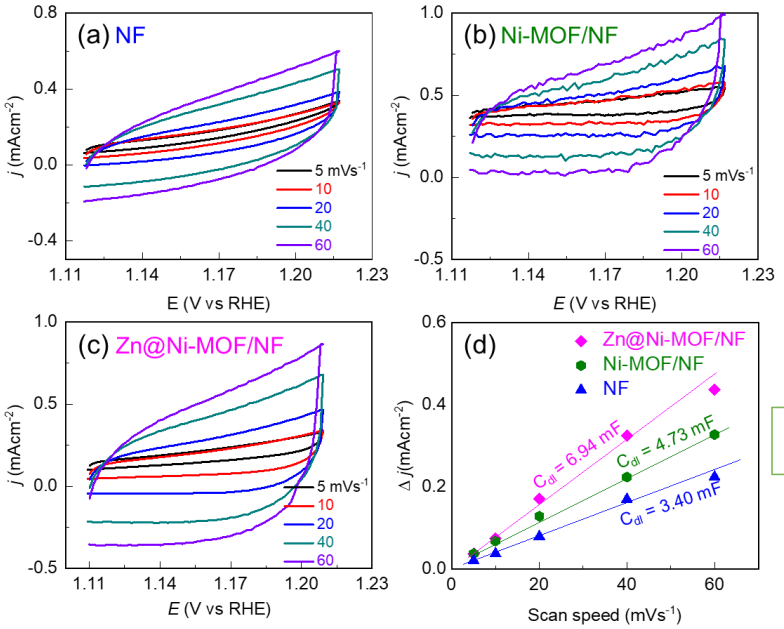

(e)

Electrode	C_{dl} (mFcm^{-2})	ECSA
NF	3.40	85.00
Ni-MOF/NF	4.73	118.25
Zn@Ni-MOF/NF	6.94	173.50

Figure S11. (a)-(c) Cyclic voltammograms of various electrodes in 0.33 M urea containing 1.0 M KOH aqueous electrolyte at different potential scanning rates (mVs^{-1}). (d) Linear plots obtained by plotting the average current density (Δj) vs potential scanning rates at 1.17 V vs RHE. (e) C_{dl} and ECSA computed from figure (d).

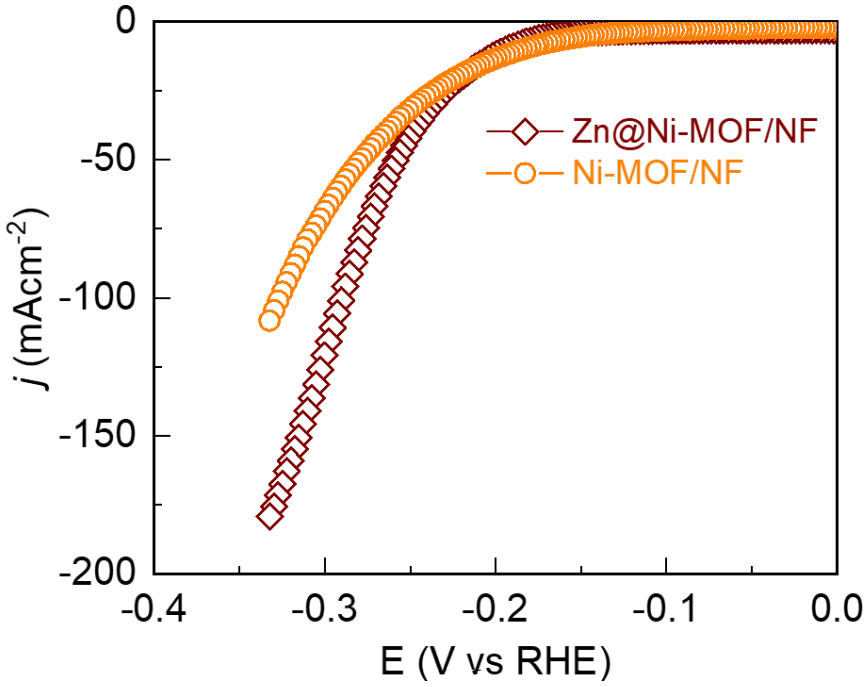

Figure S12. Cathodic linear sweep voltammetry curves of the catalytic electrodes in 1.0 M KOH aqueous electrolyte containing 0.33 M urea.

Table S1. Comparison of UOR performance for the Zn@Ni-MOF/NF with respect to reported high-performance UOR electrocatalysts (including MOF-based UOR catalysts).

Catalyst materials	**Electrolyte** 1.0 M KOH + urea	***j*** **($mAcm^{-2}$)**	**UOR potential (V) vs RHE**	**Stability**	**Reference**
NiFeRh-LDH	+ 0.33 M	10 100 240	1.34 1.47 1.59*	100 h@ 50 $mAcm^{-2}$	[1]
NiS@Ni_2S/$NiMoO_4$	+ 0.5 M	10 100 450	1.30 1.46* 1.78*	40 h@ 20 $mAcm^{-2}$	[2]
NFHC	+ 0.5 M	10 100	1.37 1.40	12 h@ 80 $mAcm^{-2}$	[3]
NiMoO-Ar/NF	+ 0.5 M	10 100 300	1.37 1.42 1.52*	100 h@ 80 $mAcm^{-2}$	[4]
CoS_2-MoS_2/NF	+ 0.5 M	10 100 350	1.29 1.33* 1.35*	30 h@ 10 $mAcm^{-2}$	[5]
CoMn/$CoMn_2O_4$	+ 0.5 M	10 100	1.32 1.36	16.6 h@100 $mAcm^{-2}$	[6]
Co(OH)F/NF	+ 0.7 M	10	1.25	10 h@ 10 $mAcm^{-2}$	[7]
NiCoP/CC	+0.5 M	10 100	1.30 1.57	30 h@ 20 $mAcm^{-2}$	[8]
AC-$Co_2(OH)_3Cl$-V-0.1	+0.33 M	30	1.54	110 h@ 20 $mAcm^{-2}$	[9]
Ni@NCNT-3	+ 0.5 M	10	1.38	10 h@ 10 $mAcm^{-2}$	[10]
hcp-CoNi-N/C	+0.33 M	10	1.31	65 h@ 10 $mAcm^{-2}$	[11]
Ni-Ni_3P@NPC/rGO	+ 0.5 M	10 100	1.35 1.42	12.5 h@ 60 $mAcm^{-2}$	[12]
Ni_2P/MoO_2/NF	+ 0.5 M	10 100	1.35 1.39	20 h@ 100 mAcm-2	[13]
MOF-based UOR catalysts					
NC-PB@CNT	+ 0.33 M	100	1.41	10 h@ 100 $mAcm^{-2}$	[14]
NiIr-MOF/NF	+ 0.5 M	10 100 300	1.33* 1.35 1.35*	15 h@ 10 mAcm-2	[15]

NiCoPx@NiFeCo-MOF/NF	+ 0.5 M	10 100 500	1.27* 1.37 1.58*	45 h@10 $mAcm^{-2}$	[16]
Ni-MOF	+ 0.33 M	10 100	1.36 1.56*	10 h@ 20 $mAcm^{-2}$	[17]
CeO_2/Ni-MOF	+ 0.33 M	10 100	1.35 1.44*	10 h@ 10 $mAcm^{-2}$	[18]
Fc-NiCo-BDC	+ 0.33 M	10 100	1.35 1.44	11 h@ 10 $mAcm^{-2}$	[19]
$NiCo_2O_4$@Ni-MOF/NF	+ 0.5 M	10 100 400	1.27 1.31 1.32	-	[20]
Ni-DMAP-t/NF	+ 0.5 M	10 100 400	1.34 1.45 1.75	10 h@ 100 $mAcm^{-2}$	[21]
Ni-bza-900	+ 0.33 M	10 100	1.38 1.71*	-	[22]
NiFe-MIL-53-NH_2	+ 0.33 M	50	1.398	20 h@ 50 $mAcm^{-2}$	[23]
Zn@Ni-MOF/NF	+ 0.33 M	10 100 500 1000 1500 1780	1.31 1.32 1.37 1.44 1.50 1.52	24 h@10 $mAcm^{-2}$ + 24 h@100 $mAcm^{-2}$	**This work**
Ni-MOF/NF	+ 0.33 M	10 100 500	1.34 1.36 1.44	24 h@10 $mAcm^{-2}$	**This work**

* UOR potential estimated from the linear polarization curves of the respective reported works.

SI-References

[1] H. Sun, W. Zhang, J.G. Li, Z. Li, X. Ao, K.H. Xue, K.K. Ostrikov, J. Tang, C. Wang, Appl. Catal. B Environ. 2021, **284**, 119740.

[2] L. Sha, T. Liu, K. Ye, K. Zhu, J. Yan, J. Yin, G. Wang, D. Cao, J. Mater. Chem. A. 2020, **8**, 18055.

[3] Y. Feng, X. Wang, P. Dong, J. Li, L. Feng, J. Huang, L. Cao, L. Feng, K. Kajiyoshi, C. Wang, Sci. Rep. 2019, **9**, 15965.

[4] Z.-Y. Yu, C.-C. Lang, M.-R. Gao, Y. Chen, Q.-Q. Fu, Y. Duan, S.-H. Yu, Energy Environ. Sci. 2018, **11**, 1890.

[5] C. Li, Y. Liu, Z. Zhuo, H. Ju, D. Li, Y. Guo, X. Wu, H. Li, T. Zhai, Adv. Energy Mater. 2018, **8**, 1801775.

[6] C. Wang, H. Lu, Z. Mao, C. Yan, G. Shen, X. Wang, Adv. Funct. Mater. 2020, **30**, 2000556.

[7] M. Song, Z. Zhang, Q. Li, W. Jin, Z. Wu, G. Fu, X. Liu J. Mater. Chem. A, 2019, **7**, 3697.

[8] L. Sha, J. Yin, K. Ye, G. Wang, K. Zhu, K. Cheng, J. Yan, G. Wang, D. Cao, J. Mater. Chem. A, 2019, **7**, 9078.

[9] B. Zhang, C. Pan, H. Liu, X. Wu, H. Jiang, L. Yang, Z. Qi, G. Li, L. Shan, Y. Lin, L. Song, Y. Jiang, J. Chem. Eng. 2022, **439**, 135768.

[10] Q. Zhang, F. MD. Kazim, S. Ma, K. Qu, M. Li, Y. Wang, H. Hu, W. Cai, Z. Yang, Appl. Catal. B-Environ. 2021, **280**, 119436.

[11] P. Li, Y. Huang, X. Ouyang, W. Li, F. Li, S. Tian, Chem. Eng. 2023, **464**, 142570.

[12] G. Li, J. Wang, J. Yu, H. Liu, Q. Cao, J. Du, L. Zhao, J. Jia, H. Liu, W. Zhou, Appl. Catal. B-Environ. 2020, **261**, 118147.

[13] M. Yang, Y. Jiang, M. Qu, Y. Qin, Y. Wang, W. Shen, R. He, W. Su, M. Li, Appl. Catal. B-Environ, 2020, **269**, 118803.

[14] S.A. Patil, S. Cho, Y. Jo, N.K. Shrestha, H. Kim, H. Im, Chem. Eng. J. 2021, **426**, 130773.

[15] Y. Xu, X. Chai, T. Ren, S. Yu, H. Yu, Z. Wang, X. Li, L. Wang, H. Wang, Chem. Commun. 2020, **56**, 2151.

[16] C. Chen, L. Jin, L. Hu, T. Zhang, J. He, P. Gu, Q. Xu, J. Lu, J. Colloid Interface Sci. 2022, **628**, 1008.

[17] D. Zhu, C. Guo, J. Liu, L. Wang, Y. Du, S.Z. Qiao, Chem. Commun. 2017, **53**, 10906.

[18] X. Wang, S. Song, H. Zhang, Mater. Lab. 2022, **1**, 220009.

[19] M. Li, H. Sun, J. Yang, M. Humayun, L. Li, X. Xu, X. Xue, A. Habibi-Yangjeh, K. Temst, C. Wang, Chem. Eng. J. 2022, **430**, 132733.

[20] Z. Dai, X. Du, X. Zhang, Int. J. Hydrogen Energy. 2022, **47**, 17252.

[21] H. Jiang, S. Bu, Q. Gao, J. Long, P. Wang, C.S. Lee, W. Zhang, Mater. Today Energy. 2022, **27**, 101024.

[22] J.L. Liu, X.Y. Zhou, J.L. An, Y.Q. Wang, M.D. Zhang, L. Qin, Energy and Fuels. 2022, **36**, 10346.

[23] Z. Gao, Y. Wang, L. Xu, Q. Tao, X. Wang, Z. Zhou, Y. Luo, J. Yu, Y. Huang, Chem. Eng. J. 2022, **433**, 133515.